Case Studies in Thermal Engineering 39 (2022) 102438

Contents lists available at ScienceDirect

Case Studies in Thermal Engineering

journal homepage: www.elsevier.com/locate/csite

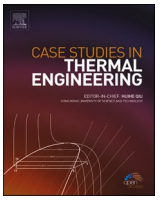

Development and performance evaluation of solar heating system for biogas production process

Dawit Gudeta Gunjo [a], Vinod Kumar Yadav [b,*], Devendra Kumar Sinha [a], Ibrahim E. Elseesy [c,d], Gulam Mohammed Sayeed Ahmed [a,e], Mostafa A.H. Abdelmohimen [c,f]

[a] Department of Mechanical Engineering, School of Mechanical, Chemical and Materials Engineering, Adama Science and Technology University, Adama, Ethiopia
[b] Department of Mechanical Engineering, G. L. Bajaj Institute of Technology and Management, Greater Noida, India
[c] Mechanical Engineering Department, College of Engineering, King Khalid University, Abha, 61421, Saudi Arabia
[d] National Research Centre, Solar Energy Department, El-Bohooth St., 12622, Giza, Egypt
[e] Center of Excellence (COE) for Advanced Manufacturing Engineering, Program of Mechanical Design and Manufacturing Engineering, School of Mechanical, Chemical and Materials Engineering, ASTU, Adama, Ethiopia
[f] Shoubra Faculty of Engineering, Benha University, Cairo, 11629, Egypt

ARTICLE INFO

Keywords:
Solar collector
Thermophilic microbes
CFD
Absorber plate
Thermal efficiency

ABSTRACT

The breakdown of organic waste, through anaerobic digestion, is a temperature dependent process. Attaining the temperature required for this process, under normal conditions, is a challenging task. Hence, the development of an effective heating system is necessary. In this paper, a solar heater's computational fluid dynamics (CFD) model, with water as working fluid, is prepared to estimate the temperatures of the absorber plate and that of the water available at the outlet. The validations of the numerical results were done by conducting experimental trials and a fair agreement between them was observed. For the examined solar collector, with outlet temperature of 61°C, the maximum thermal efficiency was estimated as 71%. The effects of operating parameters (like transmissivity coefficient, ambient temperature, wind speed, inlet water temperature and sun's insolation), were explored. It was predicted that 30–60°C tank water temperature can be attained at flow rates of 0.00833, 0.0167, and 0.021 kg/s. The bent-tube Flat Plate Colector (FPC) model, proposed in the present work, increases the residence time of water in the collector. It also increases the outlet temperature. Hence, the developed FPC model may be considered as an alternative solution for growing thermophilic bacteria during the anaerobic digestion in biogas production.

1. Introduction

Due to the surge in international oil prices, the world is looking for inexpensive energy resources of non-conventional nature (like wind, biomass, solar, nuclear, geothermal etc.). Solar thermal resources provide approximately 1701012 kW of energy to the world [1]. Because of its potential benefits in residential water heating systems, these energy sources have attracted the interest of

* Corresponding author.
E-mail addresses: dawitphd@gmail.com (D.G. Gunjo), vinod.yadav@glbitm.ac.in (V.K. Yadav), ds3621781@gmail.com (D.K. Sinha), ieelseesy@kku.edu.sa (I.E. Elseesy), gmsayeed.ahmed@astu.edu.et (G.M. Sayeed Ahmed), mostafa.abdelmohimen@feng.bu.edu.eg (M.A.H. Abdelmohimen).

https://doi.org/10.1016/j.csite.2022.102438
Received 10 June 2022; Received in revised form 7 September 2022; Accepted 17 September 2022
Available online 19 September 2022

investigators and engineers in last 20 decades [2]. Solar water heating has reduced the residential water heating expenditures by up to 70% [3]. The flat plate collector (FPC) is regarded as the most efficient and simple technology for converting solar energy into heat [4]. The fundamental FPC is made up of glass (plastic) cover, absorber plate, and a metal box (sealed). FPCs have the ability to heat the circulating fluids to temperature up to 80°C [5]. As a result, using sun's energy for water heating, the solar heating system may be considered as a critical source. As the rise in the temperature is small, simple configuration, with less maintenance, can be employed [6,7]. Bilgen and Bakeka [8] designed a solar water heating system and estimated its efficiency and cost for optimum design. Janjai et al. [9] experimentally examined the thermal behavior of manufactured plastic solar collectors. Zambolin and Col [10] conducted a comparative research study of solar water heaters (evacuated tubes) and flat plate collectors. Whiller [11] and Wijeysundera and Iqbal [12] underlined the influence and benefits of plastic covers on thermal efficiency. Njomo and Michel's [13] studied the effect of number of covers (i.e., glazing) on thermal efficiency and reported an increase in efficiency by increasing the number of covers. Agarwal and Larson [14] discovered that double glazed collectors outperformed single-glazed FPCs in terms of thermal performance due to lesser heat loss. Gunjo et al. [15] conducted a theoretical examination of the effect of surrounding conditions on the efficacy of the collectors and observed improved thermal performance with drop in heat loss factor. Yeh et al. [16] investigated the effect of aspect ratio of the collector on the thermal performance and observed that larger collector aspect ratios result in better thermal performance. In recent years, researchers use a variety of methodologies to investigate the effect of input parameters over the solar collector's performance. Akhtar and Mullick [17,18] devised an expression to calculate the temperature of one layer glazed solar collector and approximated the temperature of double-glazed solar collector glass. Gorla [19] examined the solar collector's performance using 2D finite element method technique. Hottel and Woertz [20] estimated the heat transmission rate in an FPC using lumped analysis. Duffie and Beckman [1] employed lumped analysis to develop the formula for fluid and absorber plate temperature. Amer et al. [21] studied the effect of tilt angle and inlet water temperature on collector performance using transient testing technique. Selmi et al. [22] applied computational analysis to estimate output water temperature and claimed a reasonable agreement with experimentally measured data. Kumar and Saini [23] created a solar-air-heater model and validated it with CFD results for laminar and turbulent conditions. Mohammad [24] and Gertzos et al. [25] created a computational model that fairly assessed the thermal efficiency of the model. Sultana et al. [26] used CFD to improve the design of a solar water heater in order to maximize its efficiency and estimate the coefficient of convection. Zhu et al. [27] measured the heat over the exterior of an absorber plate and compared their findings with CFD data. CFD simulation was used by Al-Ansary and Zeitoun et al. [28] to evaluate the convection as well as conduction heat loss that comes in picture with trough collectors of parabolic configuration. Faco [29] studied the flow rates inside the headers and risers using both experimental and CFD methods. It was reported that the bulk of the estimates of the performance of a solar collector may be done numerically or empirically. The use of computational techniques prior to trials could reduce the number of experimental procedures as well as the amount of time spent on them. Hence, the goal of this research is to create FPC of bent tube nature and to use it as a heat source in a biogas producing unit. The breakage of the organic wastes in biogas digesters occurs in a wide temperature range to ensure anaerobic digestion by the bacterial action. The microbes that comes in picture are: (i) phsycrophic microbes, which require temperatures below 20° Celsius, (ii) mesophilic microbes that require temperatures ranging from 30° Celsius to 45° Celsius, and (iii) thermophilic microbes, which require temperatures ranging from 50° Celsius to 60° Celsius. According to Gunjo et al. [30], because the highest outlet water temperature, obtained using FPC containing straight tube, was 50.8 °C, which in turn will not be able to meet the temperature requisite for thermophilic microbe growth. However, it may be viewed as a viable substitute for the development of the mesophilic bacteria. As a result, building a collector of flat-plate type, with suitable geometrical configuration, is the need of the hour to deliver the requisite range of temperature for thermophilic microbe digestion. The developed bent-tube FPC model is examined computationally and experimentally using water as the working fluid. This collector, when used in homes or building can lower the cost incurred with domestic water heating requirements. Vengadesan and Senthil [31], in their review, described that the shape of the heat exchangers play crucial role in enhancing the heat transfer. Neil and Sobhansarbandi [32] observed that U-Pipe setup attains higher water temperature compared to the heat pipe evacuated tube solar setup. They further reported that by using nano-PCM, the heat release gets slowed down resulting in extension of the useful period of LHS storage potential. More discussions on the shapes were also presented by Refs. [33–37], however, the discussions on the bent tube, used in the present work, is limited. The authors [38–40]

Table 1
Detailed specifications of the collector.

Collector parameters	Specifications
Absorber plate width (m)	1.00
Absorber plate's conductivity (W/m K)	386
Plate material's density (kg/m^3)	8954
Thickness of the plate (m)	0.0005
Thickness of Header and riser pipe (m)	0.0007
Quantity of glass	1
Absorber plate and glass gap (m)	0.05
Material for insulation	Glass wool
Insulating material thermal conductivity (W/m K)	0.044
Insulating material thickness (m)	0.04
Insulation material density (kg/m^3)	200
Configuration	Tube and fin
Glazing material's thickness (m)	0.03
Collector's geographic location	Guwahati (India) 26° N and 91.7° E

have done experimental and numerical analysis of LHS devices using different materials. In this paper, a computational model, for single bent connected plate, was created to estimate the temperature of the absorber plate and the outlet water, and the outcomes were validated with measurements. Steady state numerical simulations were performed utilizing the averages of the measured data from the entire day experiment in 1 h interval. Experiments were conducted for open as well as close loop heating systems in various environmental circumstances in Guwahati (India).

2. Methodology

The header and riser tube system is made up of ten bent tubes stacked in parallel. Drilling and brazing are used to attach the risers to the headers. The top of the collector was coated with acrylic glass, which is a thermoplastic with 92% transparency, and has good optical qualities with high electrical resistance. The acrylic glass was joined to the collector side with an aluminum frame. The gap between the plate and the glass is kept as small as possible to reduce overall heat loss coefficient. To improve the heat transmission properties, a thin copper absorber plate is soldered over the riser tubes. The absorber plate's surface was washed to remove dust and then painted with black ink to boost absorptivity. To limit the heat loss from the collector, sides as well as back of the collector were shielded with glass-wool. The complete specifications of the collector are shown in Table 1. The header tube and bent riser layout for the examined FPC is depicted schematically and photographically in Fig. 1.

2.1. Experimental technique

The specifications (Fig. 1) are: $L = 1.6$ m, $L_1 = 0.1$ m, $L_2 = 1.1$ m, $L_3 = 0.01$ m, $D_1 = 0.025$ m, $D_2 = 0.0125$. Fig. 2 shows the direct photographic view of the experimental facility, which depicts several sections of the solar collector as well as the essential parts of the apparatus. The reservoir supplies cold water to collector in this system. As cold water passes through the collector, it absorbs heat which results in rise in temperature. Forced circulation transports the heated water from the collector to the LHS (Latent Heat Storage) system. The thermostat installed on the biogas tank allows the liquid to move from the collector side to the biogas tank at a specified temperature. The thermostat activates a solenoid installed between the biogas tank and the LHS. When the water attains the set temperature, which is controlled through a thermostat, the solenoid valve opens and water flows from the collector side to the biogas storage tank through LHS. The heat is then transferred to the shell tank inside the heat exchanger which in turn raises the temperature of the fluid in shell tank. In the similar way, when the storage tank's temperature exceeds the set range, the water coming out of the collector flows through the shell and tube LHS system before being diverted to the reservoir by the solenoid valve.

The system drawn in Fig. 2 was designed particularly for solar water heating in applications where biogas is produced. The experiments were conducted with heat exchangers (shell and tube) in absence of filling material. Also, the controls like solenoid or thermostats were not used to test the performance before and after executing the plan. Open loop systems, containing galvanized iron pipes, were used to connect the storage tank (cold water) to the FPC's input. The solar collector's outlet pipe was linked to the heated water tank. Cold water enters the FPC from the base of the header pipe and departs from the top of the header pipe. The inlet water is heated as it circulates through the riser. The hot water is kept inside the hot water tank. T-type thermocouples were used to measure the temperatures of the water at outlet, inlet, and that of the absorber plate, glass and surroundings. Pyranometer and rotameters were used to measure the solar insolation (I) and flow rates. The thermometers and pyranometer were linked to a data capturing system (Agilent-34972 A) with a twenty-channel multiplexer that measures the temperature and solar intensity after every 10 s. The collector was installed at latitudes of 26.3°N and longitudes of 91.7°E. The experiments were conducted in the month of June 2016.

3. CFD modeling

The heater's outlet temperature and the absorber plate temperatures were predicted by the temperature distribution and flow analysis of the riser tube. Due to laminar nature, the flow was uniform with homogeneous distribution of the temperature inside the riser tubes [29]. In the present work, the laminar flow with flow rates of 30, 60, and 75 L per hour was considered. To predict the exit water and absorber plate temperature, a computational model was developed for one bent tube that is fitted over the absorber plate.

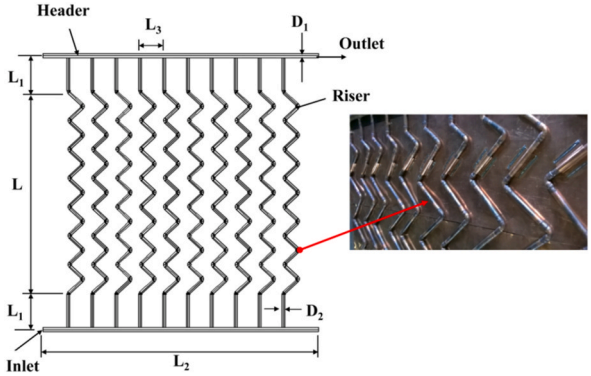

Fig. 1. Configuration used in the present work.

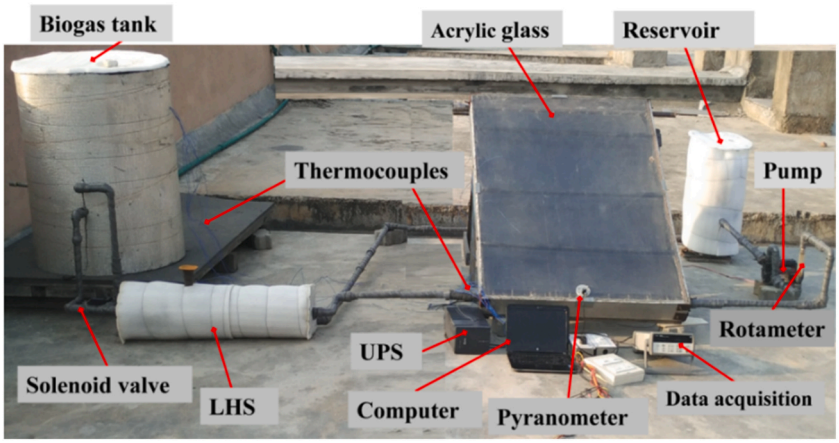

Fig. 2. Experimental facility.

For this model, the inflow water velocity for every individual riser tube analyzed was $1/10^{th}$ of the overall flow rates. ANSYS Fluent 14.5 version was used to run the simulations. The assumptions made are: water is treated as incompressible, steady and continuous. The details of the governing equations and computational procedure were kept in synchronization with author's own work [30]. Finite volume method (FVM) was used to solve the energy and momentum equations. Pressure and velocities were coupled using simple algorithms. Second order upwind scheme was used to discretize the momentum and energy equation. The velocity and the pressure outlet boundary conditions were used at the inlet and outlet. The computational domain was modeled with solid work and meshed with ANSYS CFD. Before starting the study, the grid independence test was done on the bent tube collector. The convergence is proven to be effective when the total residuals are less than 10^{-6}. Further refining was not necessary because the result changed by less than 1.54%. The bent tube connected plate model is made of 1300000 million parts, including water, absorber plate and water tube. Fig. 3a–b shows the model and meshing details.

3.1. Power required for pumping

The fluid is flowing through the collector tubes as a result of thrust created using the pump. Because the pump requires power, it becomes necessary to evaluate the total energy requirement of the pump to maintain a steady flow. In addition, it also becomes necessary to determine drop of pressure in order to calculate the pumping power. The pressure drop (Eq. (1)) is determined as per the relations proposed by Refs. [30,34,35]. The pumping power (P) was calculated using the expression proposed by Garg and Agarwal 1995 [34] and Balaji et al., 2017 [35].

$$P = m^{*}\Delta p / \rho \tag{1}$$

Where, m is the mass flow rate, Δp is the pressure drop and ρ is the density of the fluid used.

3.2. Uncertainty

Uncertainty occurs due to a variety of reasons, including reading, calibration, observation, sensitivity, drift etc. During the experimental process, the temperature of the water at various positions, ambient air temperature, mass flow rates of water, and the solar intensity were all measured independently. Table 2 shows the values of uncertainty in the independent variables. The uncertainties presented in Table 2 are calculated using the expressions proposed by Ref. [35]. The maximum uncertainty in water temperature measurement was observed as 0.2 °C.

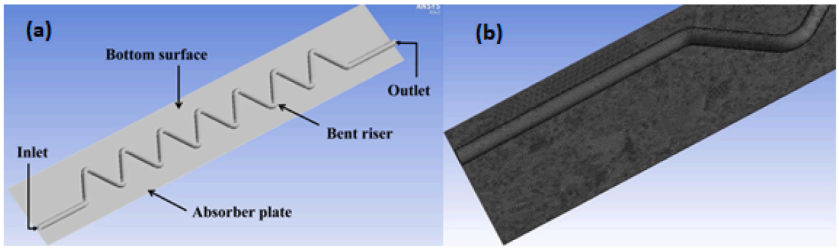

Fig. 3. (a) Bent tube and plate (b) Mesh created.

Table 2
Values of uncertainty.

Uncertainty parameters	Value (±)
Tube dia. (mm)	0.006
Temperature	0.2°C
Solar radiation estimate	5 W/m^2
Mass flow rate (water)	4 kg/s
Reynolds number	2.83%
Thermal efficiency of heating system	3.8%
Wind speed	4.0%

4. Results and discussion

The simulations adopted in the model are based on steady-state that computes the average values of the acquired data during an interval of 1-h. The experimental data like ambient temperature, inlet water temperature (Ti), solar insolation, and the mass flow rates were applied on the created model. Fig. 4a–c shows the variation in measured solar insolation on hourly basis, ambient temperature (Ti). The flow rates were maintained at 30, 60, and 75 L per hour. The measured results of Fig. 4a–c reveal that the average solar insolation (I) rises from 8:00 a.m. and reaches its highest between 11:00 a.m. and 12:00 noon. The reservoir tank was insulated in order to regulate the inlet water's temperature rise. This also ensures more absorption of heat during peak hours. For entire range of flow rates studied, the changes in the inlet water temperature corresponds to 4 K only. Experiments conducted after 04:00 p.m. result in a drop in I, Ta, and Ti.

4.1. Model validation

The validation was done by comparing the computed findings with the experimental results. Fig. 5a depicts the disparity of CFD results of water temperature at outlet alongside the bent tube when the flow rate was 0.0083 kg/s. The changes in the water temperature across bent tube length at 12:00 noon (Fig. 5a) indicate that the upper portion of the tube has greater exit water temperatures than the bottom portion. Because the fluid enters the collector at the lower end, the temperature at the upper end was higher than the temperature at the lower end. The simulation's inlet settings were: I = 925 W/m^2, Ti = 309 K and Ta = 307.6 K.

Fig. 5b depicts the distribution of the temperature at the outer tube diameter at 12:00 noon. As tube's one half part is brazed with absorber plate, the surface temperature was higher than that of the tube's Centre temperature. The heat gets transferred through

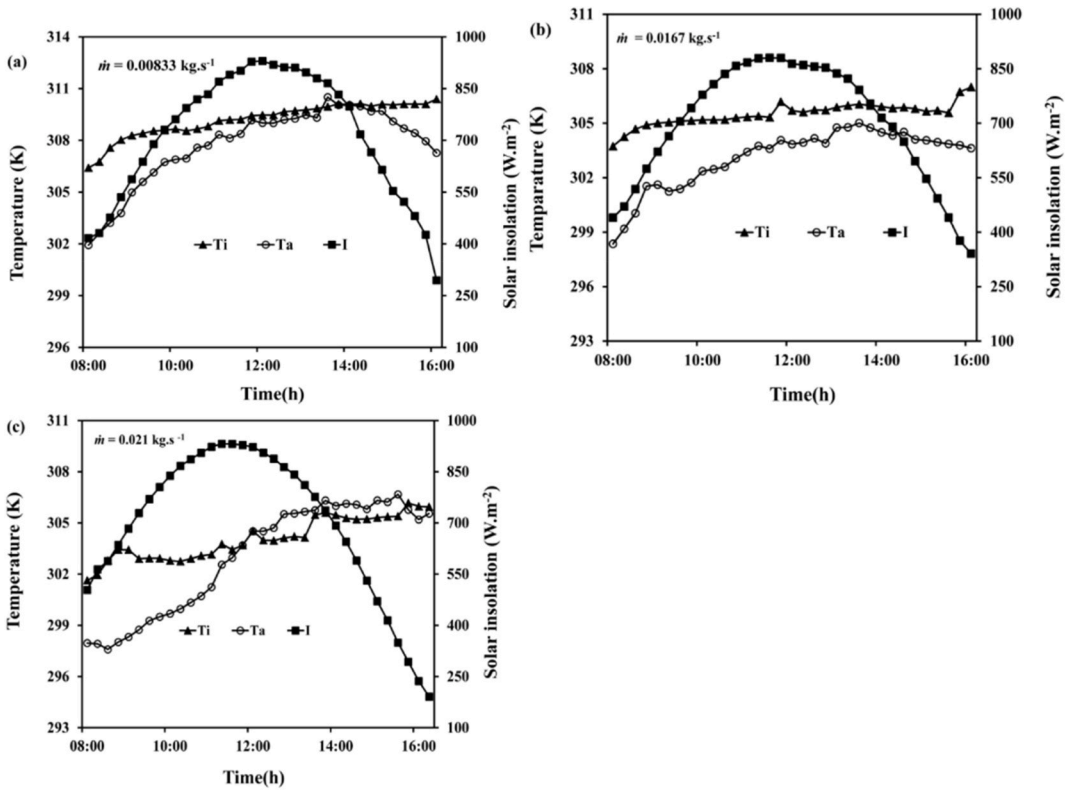

Fig. 4. Variation of I, T_i, T_a as a function of time.

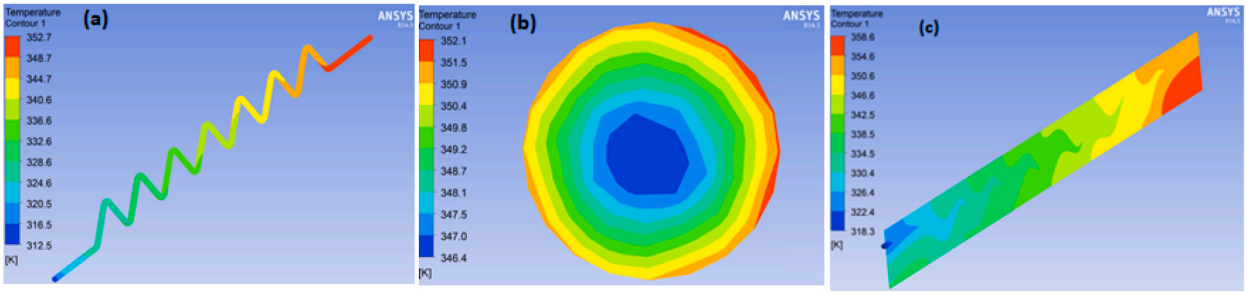

Fig. 5. Temperature distribution at 12.00 noon (a) tube (b) water outlet (c) absorber plate.

combined modes of radiation, conduction (tube thickness), and convection (within tube). As heat transfers from the surface to the mid-tube, it takes more time (through convection). The temperature of the water at the mid of the tube is less than that of surface temperature by 6 K. Fig. 5c displays the temperature distribution of the absorber plate at 12:00 noon. Temperature distribution along absorber plate length suggests a 38 K drop between the intake and exit sides of the plate. Since, cold fluid absorbs heat within the riser tube that comes in close vicinity with the absorber (at mid-section); there occurs a 6 K variance over the plate width. High exit water and low absorber plate temperatures were noticed when the fluid passed through the bent tube.

4.2. Comparison of experimental and simulated results of water at exit

Fig. 6a 6(b), and 6(c) shows the comparative results of simulation and experimental observations (flow rates: 0.0083, 0.0167 and 0.021 kg/s respectively). The experimental and computational results show that for lower flow rates, the outlet water temperature is higher than that for higher flow rates. Although, the computed results are higher than measured results, the distribution with time follows a similar pattern. The percentage variation between these two sets was calculated using the relations proposed by Wei et al. [36]. The comparative results illustrates that experimental as well as simulated results follow similar trend, and the maximum errors are 3.5%, 3.1% and 4.8% at flow rates of 0.00833, 0.0167 and 0.021 kg/s respectively. The results also show that the created model is capable of estimating the exit water temperature with 5% error at all flow rates used in the present work. The maximum and minimum outlet water temperatures for collector was 332 K (at 0.0083 kg/s) and 319 K (at 0.021 kg/s) respectively. The results conceal that the experimentally measured outlet water temperature rise is smaller than the computed results with increased intensity of solar insolation. As a result, the errors were at their peak during peak solar insolation. Because the results were influenced by the weather conditions throughout the experiments, precise determination of the convection heat loss coefficient throughout the day was unattainable. However, the average convection coefficient was used for the whole day. As a result, the error in case of peak solar insolation seems to be the highest in all scenarios (see Fig. 7).

Fig. 8a depicts the temperature difference between cold and hot water for the selected mass flow rates. It can be observed that with 0.0083 kg/s flow rate, the temperature changes are highest compared to other flow rates maintained in this work. For mass flow rates of 0.0083, 0.0167, and 0.021 kg/s, the major temperature differences (daily average) were 10.68, 5.64 K and 5.2 K respectively. The heat transported per unit water volume decreases as the flow rate through the collector increases, identical to the trend of temperature variation obtained between inlet and outlet water.

Fig. 8b depicts the variance of useable energy recovered as function of time during a sunny day. The figure demonstrated that the useable energy gain was greater at higher flow rates than at lower flow rates. The progressive rise in inlet water temperature has a negative impact on the solar heating system. Circulating hot incoming water through the collector reduces the temperature of the collector's exit water. This is due to hot water's reduced absorption rate. In the similar fashion, with an increase in solar insolation, the radiated emissions from absorber plate top surfaces also increases. This results in enhanced heat loss through convection at solar collector, and consequently less useable energy is retrieved. Hence, in this work, the water tank carrying cold water is insulated. The daily daylight's useable energy gained on per day basis was 15.3 MJ, 15.8 MJ and 18.2 MJ for the mass flow rates of 0.0083, 0.0167,

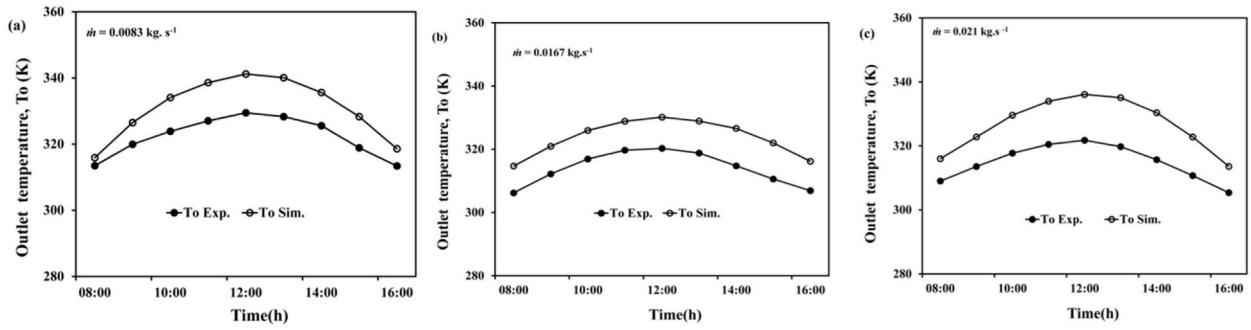

Fig. 6. Outlet water temperature distribution (kg/s) (a) = 0.0083 (b) = 0.0167 (c) = 0.021.

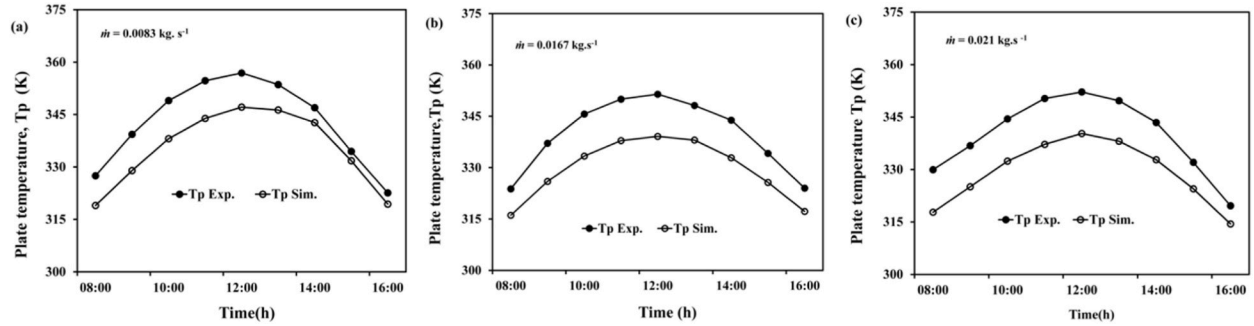

Fig. 7. (a), (b), and (c) show the fluctuation of actual and simulated findings of the plate temperature distribution at 0.0083, 0.0167, and 0.021 kg/s, respectively. The measured results indicate a constant rise in plate temperature (at 8:00 a.m.) and reaching at its peak at 12:00 noon. Thereafter, it decreases for all flow rates. The maximum as well as minimum temperature of the absorber plate was observed as 356 K (at 0.0083 kg/s) and 347 K (at 0.021 kg/s) respectively. The measured temperature (plate) was higher than the predicted results under all flow rates with 4% error. This deviation in computations is attributed to the supposition of perfect communication between the tube and the plate, which resulted in high heat rate of heat transfer (plate to fluid). Temperature variation (experiment and predictions).

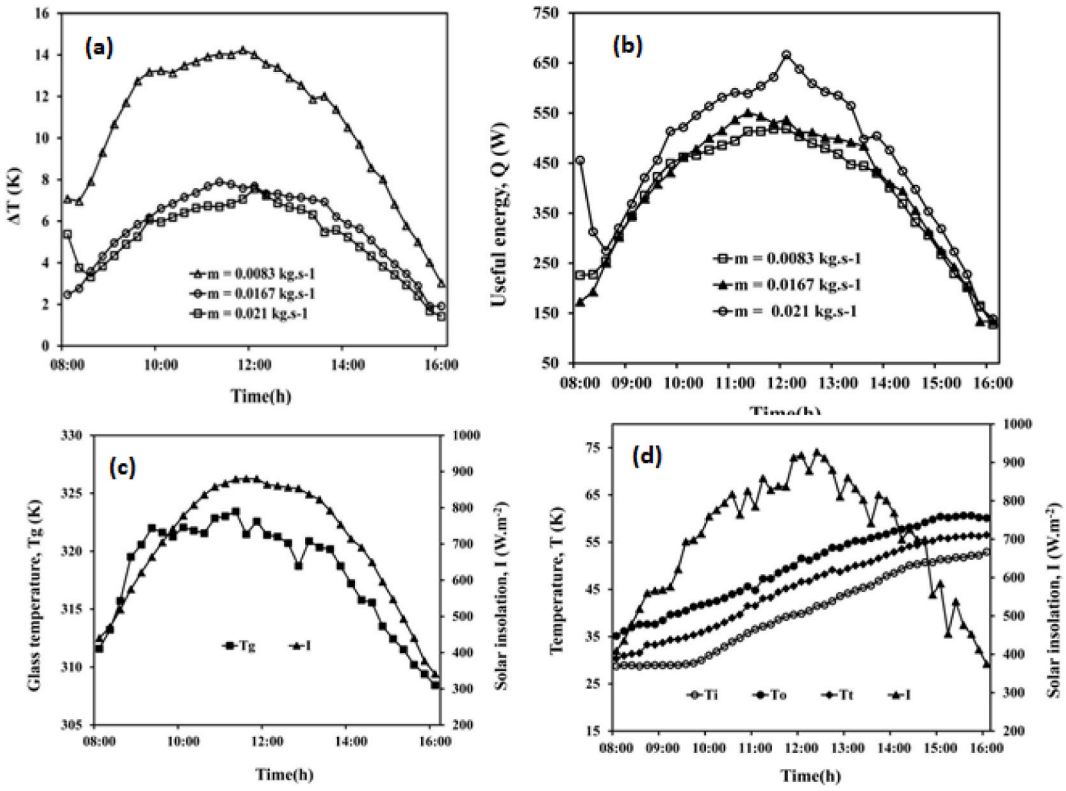

Fig. 8. (a) Temperature distribution (b) Useful energy with time at different flow rates (c) Glass temperature distribution and solar insolation (d) Measured temperature of water passing through bent tube.

and 0.021 kg/s respectively. This was calculated by adding the useful energy and multiplying it by the number of experiment hours. The full day trial findings demonstrated higher output water temperature at lower flow rate, despite the fact that the pump may be overheated when the fluid at low flow rates are passed through it.

Fig. 8c depicts the temperature fluctuations of the glass and solar insolation as a function of time. It can be inferred that the glass temperature start rising at 8:00 a.m. and attains its peak around 12.00 noon. Furthermore, as the time progresses, the sun's insolation falls. This in turn, lowers the glass temperature. The highest glass temperature was recorded as 323.5 K at an insolation of 880 W/m^2. This demonstrates that acrylic glass can withstand higher temperatures. Experimentally observed outlet water temperature (To), inlet water temperature (Ti), storage tank temperature (Tt), and the solar insolation (I) for the analyzed solar collector are shown in Fig. 8d. The solar insolation received over the collector's surface rises with time, reaching a peak of 927 W/m^2 at 12:00 noon and then it decreases. The temperature of the inflow water gradually rises from 301 to 325 K from morning to 16.00 h. The temperature of the

output water gradually rises from 307 K in the morning to 335 K in the afternoon. The temperature of the water in the tank gradually rises from 298.6 K to 325.4 K from morning to 16:00 h. The temperature of the storage tank water was considered as the average of inlet and outlet water temperature at any specific time. Because the temperature range required for growing bacteria for anaerobic digestion is in the range of 303 K–328 K, the solar water heating system, fitted with bent tubes, may be sought as an alternative approach to boost the production of biogas.

Fig. 9a depicts the experimental findings for the solar collector's (bent tube) inlet water temperature, outflow water temperature, solar insolation and thermal efficiency. The solar insolation collected over the collector's surface followed a parabolic path, reaching its peak at 12.00 noon with a maximum value of 864 W/m^2. From 8:00 a.m. to 04:00 p.m., the temperature of the inlet and outlet water increases. The temperature of the inlet water gradually rises from 28.8°C to 53°C from morning to evening respectively. Furthermore, the temperature of the output water grew steadily from 35.1°C to 61°C. Gunjo et al. [30] reported a maximum exit water temperature with straight tube collector as 50.8°C. Furthermore, the temperatures of the inlet and outlet water follow the same linear trend. About 10:30 a.m., a peak thermal efficiency of 71% was noticed. On the other hand, the thermal efficiency reported by Gunjo et al. [30] was 59% only. This proves that the bent tube collectors, with capability of growing thermophilic micro-organisms, are superior for biogas production. The results also indicate that after 02:00 p.m., the solar thermal efficiency start dropping. This is due to the reduction in the temperature difference (To – Ti) as a result of reduction in solar insolation.

The thermal efficiency of the collector is calculated using mean temperature (Tm) of water that passes through the collector, the surrounding temperature, and the amount of insolation. The collector's efficiency is calculated using loss parameter (Tm–Ta)/I. The thermal efficiency is calculated using the equation proposed by Xudong et al. [37]. Fig. 9b depicts a plot of thermal efficiency versus (Tm–Ta)/I for the collector (bent tube) as observed during experimentation. The slope and intercept of best fitting curve are 9.6 and 0.7 respectively with RMS of 0.91.

Fig. 9c depicts the deviation of friction factor and pressure drop versus mass flow rate for the examined collector (bent tube type). As can be seen, initially, the friction factor is high at the entry corresponding to higher flow rate. With an increased mass flow rate, the friction factor decreases and pressure drop increases. The adversarial pressure gradients, inside the bent tubes (just after the bend), causes flow separation. This effect causes increased pressure loss that is due to the combined effect of momentum and friction as a result of directional changes encountered while passing through a bent tube. These parameters depend upon the bend angle, the curvature ratio and the Reynolds Number. The drop in pressure at 0.0083 kg/s and 0.021 kg/s was 510 Pa and 1860 Pa respectively. For an 8-h experiment, the pump's running cost for the collector was Rupees 4.10 (INR) at 0.021 kg/s flow rate.

Fig. 9d depicts the thermal efficiency as a function of Ti with solar insolation variation (at Ta = 298 K). An increase in the efficiency of the collector was observed with decrease in the inlet water temperature. In addition, by increasing the flow rate of inflow water temperature (with constant I and Ta) the thermal efficiency drops. This decrease in the thermal efficiency is more pronounced for the lower radiation levels. It was also observed that when the sun's insolation was higher and the inlet temperature of the water was less, the collector's efficiency was higher. Fig. 9e depicts the fluctuation of the efficiency with ambient temperature with constant I and Ti of 700 W/m^2 and 303 K respectively. The efficiency changes linearly with Ta. As the temperature (Ta) rises, the heat loss of the system due to conduction, convection, and radiation mechanisms decreases. Consequently, the collector's efficiency improves. According to Fig. 9e, thermal efficiency intensifies linearly with an increase in ambient temperature. Fig. 9f depicts the fluctuation of thermal efficiency with transmissivity coefficient by adjusting gravity while keeping other parameters constant. For determining FPC efficiency, the glass cover's optical properties are necessary parameters. The results show that the thermal efficiency increases linearly with glass cover's transmissivity coefficient. Better thermal efficiency came from a higher transmissivity ratio of the glass cover. The collector's tilt angle was set as 26.7°, the plate temperature was set at 350 K, and the plate emissivity was fixed as 0.1 with glass (g = 0.9). It can be depicted that when the wind speed increases, the overall heat loss factor increases. Furthermore, as the wind velocity rises, the thermal efficiency of solar collector gets reduced as a result of increased convective heat loss. In general, the convection induced as a result of wind speed, plays a vital role for loss of heat in FPCs as they are usually located in open environment where strong winds may often be noticed based on the weather conditions. This intermittency could significantly affect the stability and the optical performance of the FPCs.

5. Conclusions

In this paper, a solar water heater, with bent tube collector, is built and was investigated numerically and experimentally. The following are the key conclusions:

a) A bent-tube FPC model, which takes water as the working medium, increases the residence time of water in the collector, increases the outlet temperature, and keeps the temperature of the tank in the range of 303–331 K. This effect is conducive for the cultivation of thermophilic anaerobic fermentation micro-organisms.
b) The variation in water temperature is greater at low flow rates than at higher flow rates.
c) The thermal efficiency of the bent tube model is higher than that of the conventional straight-tube FPC model. The maximum solar thermal efficiency of the bent tube model was 71%. In addition, the pressure drop and electricity charges required for driving the pump at 0.021 kg/s flow rate was 1975 Pascal and Rupees 4.1 (INR) respectively.
d) A parametric research demonstrates that increasing insolation, ambient temperature, and flow rate, increases the thermal efficiency. However, by decreasing the inlet water temperature and wind speed, the thermal efficiency increases.

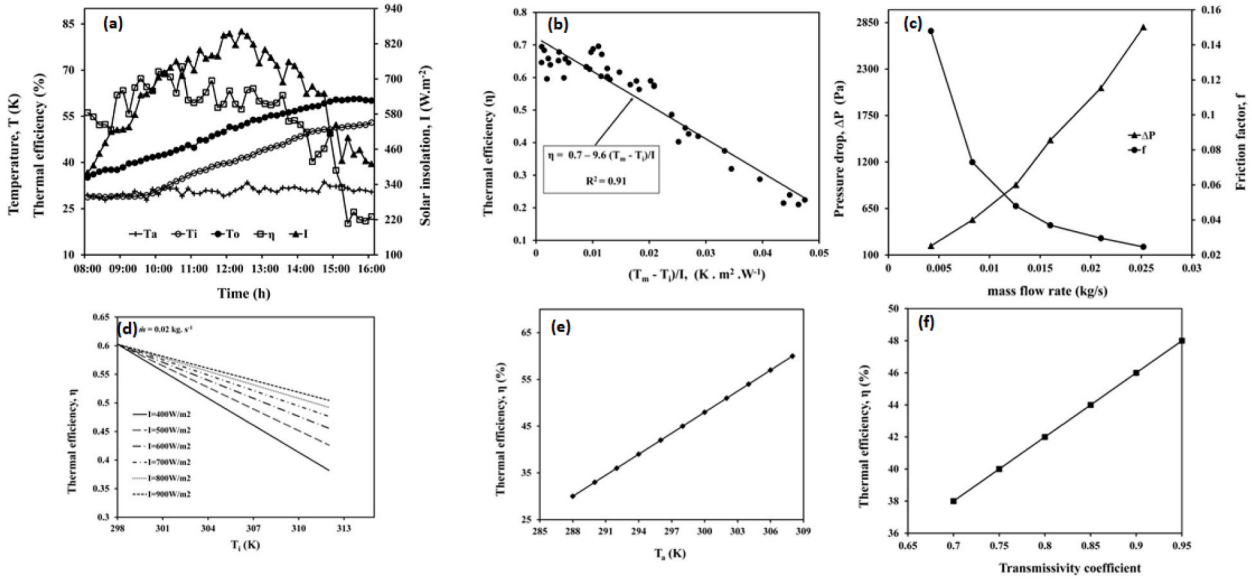

Fig. 9. **(a)** Temperature and thermal efficiency of bent tube heating system (b) Thermal efficiency and (T_m–T_a)/I relation (bent tube) (c) Pressure drop, friction factor variation with flow rate (d) Thermal efficiency, with solar insolation and inlet water temperature (e) Thermal efficiency and ambient temperature (f) Effect of transmissivity coefficient on thermal efficiency.

Funding

The authors extend their appreciation to the Deanship of Scientific Research at King Khalid University for funding this work through Large Groups (RGP.2/94/43).

Author contribution

All authors have equal contribution in the development of this paper.

Declaration of competing interest

The authors declare that they have no known competing financial interests or personal relationships that could have appeared to influence the work reported in this paper.

Data availability

Data will be made available on request.

Acknowledgement

The authors extend their appreciation to the Deanship of Scientific Research at King Khalid University for funding this work through Large Groups (RGP.2/94/43). The numerical simulations were conducted at IIT Guwahati.

References

[1] J.A. Duffie, W.A. Beckman, Solar Engineering of Thermal Process, John Willy & Sons, New York, 1991.
[2] N. Cardinale, F. Piccininni, P. Stefanizzi, Economic optimization of low-flow solar domestic hot water plants, Renewable Energy 28 (12) (2003) 1899–1914.
[3] Shelke, V.G. and Patil, C.V., Analyze the Effect of Variations in Shape of Tubes for Flat Plate Solar Water Heater.
[4] Vasudeva K. Karanth, N. Madhwesh, M.S. Manjunath, Numerical and experimental study of a solar water heater for enhancement in thermal performance, International Journal of Research in Engineering and Technology (IJRET) 4 (3) (2015) 548–553.
[5] Réné Tchinda, A review of the mathematical models for predicting solar air heaters systems, Renewable and sustainable energy reviews 13 (8) (2009) 1734–1759.
[6] Soteris Kalogirou, Thermal performance, economic and environmental life cycle analysis of thermosiphon solar water heaters, Solar energy 83 (1) (2009) 39–48.
[7] M. Keyanpour-Rad, H.R. Haghgou, F. Bahar, E. Afshari, Feasibility study of the application of solar heating systems in Iran, Renewable energy 20 (3) (2000) 333–345.
[8] E. Bilgen, B.J.D. Bakeka, Solar collector systems to provide hot air in rural applications, Renewable Energy 33 (7) (2008) 1461–1468.
[9] S. Janjai, A. Esper, W. Mühlbauer, Modelling the performance of a large area plastic solar collector, Renewable energy 21 (3) (2000) 363–376.
[10] E. Zambolin, D. Del Col, Experimental analysis of thermal performance of flat plate and evacuated tube solar collectors in stationary standard and daily conditions, Solar Energy 84 (8) (2010) 1382–1396.
[11] Austin Whillier, Plastic covers for solar collectors, Solar Energy 7 (3) (1963) 148–151.
[12] N.E. Wijeysundera, M. Iqbal, Effect of plastic cover thickness on top loss coefficient of flat-plate collectors, Solar Energy 46 (no. 2) (1991) 83–87.

[13] Donatien Njomo, Michel Daguenet, Sensitivity analysis of thermal performances of flat plate solar air heaters, Heat and mass transfer 42 (12) (2006) 1065–1081.
[14] V.K. Agarwal, D.C. Larson, Calculation of the top loss coefficient of a flat-plate collector, Solar Energy 27 (no. 1) (1981) 69–71.
[15] Dawit G. Gunjo, P. Mahanta, P.S. Robi, Impact of ambient conditions and top heat loss on useful energy of flat plate solar collectors, International Journal of Emerging Trends in Electrical and Electronics (IJETEE) 11 (2) (2015) 209–213.
[16] Ho-Ming Yeh, Chii-Dong Ho, Chun-Hung Chen, The effect of collector aspect ratio on the collector efficiency of sheet-and-tube solar fluid heaters, Tamkang Journal of Science and Engineering 2 (2) (1999) 61–68.
[17] N. Akhtar, S.C. Mullick, Approximate method for computation of glass cover temperature and top heat-loss coefficient of solar collectors with single glazing, Solar energy 66 (5) (1999) 349–354.
[18] N. Akhtar, S.C. Mullick, Computation of glass-cover temperatures and top heat loss coefficient of flat-plate solar collectors with double glazing, Energy 32 (7) (2007) 1067–1074.
[19] Rama Subba Reddy Gorla, Finite element analysis of a flat plate solar collector, Finite elements in analysis and design 24 (4) (1997) 283–290.
[20] Hoyt Hottel, B. Woertz, Performance of flat-plate solar-heat collectors, Trans. ASME (Am. Soc. Mech. Eng.);(United States) (1942) 64.
[21] E.H. Amer, J.K. Nayak, G.K. Sharma, Transient method for testing flat-plate solar collectors, Energy Conversion and Management 39 (7) (1998) 549–558.
[22] Mohamed Selmi, J. Mohammed, Al-Khawaja, Abdulhamid Marafia, Validation of CFD simulation for flat plate solar energy collector, Renewable Energy 33 (3) (2008) 383–387.
[23] Sharad Kumar, R.P. Saini, CFD based performance analysis of a solar air heater duct provided with artificial roughness, Renewable Energy 34 (5) (2009) 1285–1291.
[24] Mohamed B. Gadi, Design and simulation of a new energy-conscious system (CFD and solar simulation), Applied energy 65 (1) (2000) 251–256.
[25] K.P. Gertzos, S.E. Pnevmatikakis, Y.G. Caouris, Experimental and numerical study of heat transfer phenomena, inside a flat-plate integrated collector storage solar water heater (ICSSWH), with indirect heat withdrawal, Energy Conversion and Management 49 (11) (2008) 3104–3115.
[26] Tanzeen Sultana, Graham L. Morrison, Rosengarten Gary, Thermal performance of a novel rooftop solar micro-concentrating collector, Solar Energy 86 (7) (2012) 1992–2000.
[27] Li Zhu, Yiping Wang, Zhenlei Fang, Yong Sun, Qunwu Huang, An effective heat dissipation method for densely packed solar cells under high concentrations, Solar Energy Materials and Solar Cells 94 (2) (2010) 133–140.
[28] Hany Al-Ansary, O. Zeitoun, Numerical study of conduction and convection heat losses from a half-insulated air-filled annulus of the receiver of a parabolic trough collector, Solar Energy 85 (11) (2011) 3036–3045.
[29] Jorge Facão, Optimization of flow distribution in flat plate solar thermal collectors with riser and header arrangements, Solar Energy 120 (2015) 104–112.
[30] D.G. Gunjo, P. Mahanta, P.S. Robi, CFD and Experimental Investigation of Flat Plate Solar Water Heating System under Steady State Condition, Renewable Energy, 2016.
[31] E. Vengadesan, Senthil, A review on recent development of thermal performance enhancement methods of flat plate solar water heater, Solar Energy 206 (2020) 935–961.
[32] Tyler J.E. O'Neil, Sarvenaz Sobhansarbandi, Thermal performance investigation of energy storage based U-pipe evacuated tube solar collector: an experimental study, Sustainable Energy Technologies and Assessments 52 (2022), 102146. Part B.
[33] M. Kahani, S.Z. Heris, S.M. Mousavi, Effects of curvature ratio and coil pitch spacing on heat transfer performance of Al_2O_3/water nanofluid laminar flow through helical coils, Journal of Dispersion Science and Technology 34 (12) (2013) 1704–1712.
[34] H.P. Garg, R.K. Agarwal, Some aspects of a PV/T collector/forced circulation flat plate solar water heater with solar cells, Energy Conversion and Management36 (2) (1995) 87–99.
[35] K. Balaji, S. Iniyan, Muthusamyswami, Experimental investigation on heat transfer and pumping power of forced circulation flat plate solar collector using heat transfer enhancer in absorber tube, Applied Thermal Engineering 112 (2017) 237–247.
[36] Wei He, Xiaoqiang Hong, Bingqing Luo, Hongbing Chen, Jie Ji, CFD and comparative study on the dual-function solar collectors with and without tile-shaped covers in water heating mode, Renewable Energy 86 (2016) 1205–1214.
[37] Xudong Zhao, Zhangyuan Wang, Tang Qi, Theoretical investigation of the performance of a novel loop heat pipe solar water heating system for use in Beijing, China, Applied Thermal Engineering 16 (2010) 2526–2536.
[38] D.G. Gunjo, V.K. Yadav, D.K. Sinha, M.A. Elkotb, G.M.S. Ahmed, N. Hossain, M.A.H. Abdelmohimen, Improvement in thermal storage effectiveness of paraffin with addition of aluminum oxide nanoparticles, Materials 15 (13) (2022) 4427.
[39] Dawit Gudeta Gunjo, Vinod Kumar Yadav, Devendra Kumar Sinha, H.A. Refaey, Gulam Mohammed Sayeed Ahmed, Mostafa A.H Abelmohimen. Performance of latent heat storage (LHS) systems using pure paraffin wax as working substance. Case Studies in Thermal Engineering, 39 (2022):102399.
[40] Dawit Gudeta Gunjo, Vinod Kumar Yadav, Devendra Kumar Sinha, Performance analysis of latent heat storage systems using CuO nanoparticles, Evergreen - Joint Journal of Novel Carbon Resource Sciences & Green Asia Strategy 9 (2) (2022) 292–299.